Mean field equilibria of single coherent vortices

Peilong Chen* and M. C. Cross†
Condensed Matter Physics 114-36, California Institute of Technology, Pasadena, California 91125
(Received 19 July 1996)

We present the calculation of single-vortex statistical equilibria in a disk using the mean field theory respecting all the conservation laws of the two-dimensional Euler equations. The equilibrium may help in understanding the formation of coherent structures in experiments, numerical simulations, and planetary atmospheres. We calculate two-dimensional single-vortex solutions in the disk and confirm the bifurcation from symmetric to off-center vortices predicted by a linear perturbation analysis. With a second-order perturbation analysis and a calculation of the thermodynamic stability we find that both supercritical and subcritical bifurcations can occur, depending on the parameters. The shapes of the off-center vortices also are in good agreement with measurements on an electron plasma. [S1063-651X(96)11212-5]

PACS number(s): 47.20.−k, 05.20.Gg, 52.25.Kn, 92.90.+x

I. INTRODUCTION

Two-dimensional (2D) turbulence evolution is known to be dominated by the formation of coherent vortices. Many numerical simulations and experiments [1–3] have demonstrated that the relaxation of 2D turbulence with initial small scale motion is characterized by the formation of larger and larger coherent vortices, and eventually a steady single coherent structure is reached. The large, long-lived vortices observed in planetary atmospheres are also possible examples of this process. These studies strongly suggest that the formation of large scale structures is mainly an inviscid process, and viscosity and dissipation only affect the fine scale motion. This leads to the idea of using the statistical mechanics of a 2D incompressible ideal fluid (the Euler equations) to understand these coherent structures. A statistical mechanics treatment of the Euler equations modeling the fluid as a collection of point vortices has been studied for a long time [4]. However, the point vortex model suffers from the problem that the infinity of conservation laws of vorticity integrals of the Euler equations are not respected. A statistical theory of a 2D incompressible ideal fluid respecting all the conserved quantities has been derived [5]. Based on the assumption of ergodicity constrained by the conservation laws, the final equilibrium from a given initial condition can be calculated directly without knowing the intervening dynamics and the dependence of the final states on the system parameters can be quickly studied.

Studying the single-vortex statistical equilibrium could be the first step toward understanding coherent vortex structures. Transitions from a simple shear layer to a coherent vortex have been studied [6,7] in the mean field theory with rectangular or annular geometries. Single-vortex solutions in a disk have also been investigated [8,7] using the point vortex model or the mean field theory. In these two papers symmetric single-vortex solutions at the disk center are calculated and a bifurcation to off-center single vortices is found by a linear perturbation analysis on the symmetric solutions. In this paper we solve the 2D mean field equations for both symmetric and asymmetric solutions to get a complete picture of the problem. These solutions allow us to compare the thermodynamic quantities directly and show explicitly that there is a critical energy above which the off-center vortices are thermodynamically more probable states. The shapes of off-center vortices in the 2D solutions are also compared with the results of an electron plasma experiment [9] and good agreement is found.

We also perform a second-order perturbation analysis at the bifurcation point. By extending the analysis to second order we can quickly identify the bifurcation type and understand the behavior of off-center vortices near it. Although we can also get this information by computing all 2D asymmetric solutions, the analysis is faster and free of the numerical error from discretizing the disk. Combining the nonlinear analysis results with the 2D solutions, we show that the bifurcation is always supercritical and thus a second-order transition when the system energy is varied. However, if the system temperature is used as the control parameter, a first-order transition (a subcritical bifurcation) can occur at some parameters. An interesting aspect of this first-order transition is that because of the long range vortex-vortex interaction the system will not be in a mixture of two stable states as is common in systems with short range interaction (e.g., water). Finally we use a stability analysis to calculate explicitly the thermodynamic stability property of the solutions, i.e., whether they are local entropy maxima; the stability confirms the results of the bifurcation analysis.

II. STATISTICAL EQUILIBRIUM

The dynamics of a 2D incompressible ideal fluid is described by the equation of motion:

$$\frac{\partial \mathbf{u}}{\partial t} + (\mathbf{u}\cdot\nabla)\mathbf{u} = -\nabla p. \tag{1}$$

Here $\mathbf{u}(\mathbf{r})$ is the 2D velocity field and p is the fluid pressure. The equation of mass conservation of the incompressible flow is $\nabla\cdot\mathbf{u}(\mathbf{r})=0$ and can be satisfied by introducing the stream function $\psi(\mathbf{r})$, defined as $\mathbf{u}(\mathbf{r})=\nabla\times\psi\hat{\mathbf{z}}$

*Electronic address: peilong@styx.caltech.edu
†Electronic address: mcc@styx.caltech.edu

$=(\partial\psi/\partial y, -\partial\psi/\partial x)$. Taking the curl of Eq. (1) and defining vorticity $\omega(\mathbf{r})\hat{\mathbf{z}}=\nabla\times\mathbf{u}(\mathbf{r})$ yields the equation of motion

$$\frac{\partial\omega}{\partial t}+(\mathbf{u}\cdot\nabla)\omega=0. \tag{2}$$

The stream function and vorticity are related by the Poisson equation, $\nabla^2\psi=-\omega$. Equation (2) implies that there are an infinite number of conserved vorticity integrals, $\int_{\eta(t)}f(\omega(\mathbf{r}))d\mathbf{r}$, for any path $\partial\eta(t)$ moving with the fluid and f an arbitrary function. These conserved quantities can be described by a conserved vorticity distribution function $g(\sigma)$ defined as

$$g(\sigma)\equiv\int\delta(\sigma-\omega(\mathbf{r}))d\mathbf{r}.$$

Physically $g(\sigma)$ measures the fractional area covered by the vorticity level σ. Combining $g(\sigma)$ and the Hamiltonian $H=1/2\int|\mathbf{u}(\mathbf{r})|^2d\mathbf{r}$, the statistical mechanics treatment predicts that the asymptotic large time equilibrium is given by [5]

$$n_0(\mathbf{r},\sigma)=\frac{\exp\{-\beta[\sigma[\psi_0(\mathbf{r})-h(\mathbf{r})]-\mu(\sigma)]\}}{\int_{-\infty}^{\infty}d\sigma'\exp(-\beta\{\sigma'[\psi_0(\mathbf{r})-h(\mathbf{r})]-\mu(\sigma')\})}$$

Here the coarse-grained equilibrium stream function ψ_0 and vorticity field ω_0 are determined self-consistently from n_0,

$$-\nabla^2\psi_0(\mathbf{r})=\omega_0(\mathbf{r})=\int_{-\infty}^{\infty}d\sigma\sigma n_0(\mathbf{r},\sigma).$$

The function $\mu(\sigma)$ is determined by the $g(\sigma)$ constraint:

$$g(\sigma)=\int d\mathbf{r}n_0(\mathbf{r},\sigma),$$

and the inverse temperature β is determined by fixing the energy. The function $h(\mathbf{r})$ may be used to account for external fields and other conserved quantities in geometries of special symmetry.

In this paper we solve the above mean field equations in a unit disk. We also choose for simplicity the $g(\sigma)$ corresponding to an initial vorticity distribution with only two vorticity levels, 0 and q,

$$g(\sigma)=(V-\alpha)\delta(\sigma)+\alpha\delta(\sigma-q),\quad 0\leqslant\alpha\leqslant V,$$

with V the area of the disk. In an equilibrium state the coarse-grained vorticity field $\omega_0(\mathbf{r})$ will typically take on a continuum of values, always bounded by the value q. The energy of the system is given by

$$E=\frac{1}{2}\int\psi_0\omega_0d\mathbf{r},$$

if we use the boundary condition: $\psi_0(r=1)=0$. The entropy is calculated by

$$S=-\int\left[\frac{\omega_0}{q}\ln\left(\frac{\omega_0}{q}\right)+\left(1-\frac{\omega_0}{q}\right)\ln\left(1-\frac{\omega_0}{q}\right)\right]d\mathbf{r}.$$

Finally because of the rotational symmetry of the disk, $h(\mathbf{r})$ includes a Lagrange multiplier term Ωr^2 to impose the conservation of angular momentum. With all these considerations, the mean field equations become [5]

$$\nabla^2\psi_0(\mathbf{r})=\omega_0(\mathbf{r})=\frac{q}{1+\exp\{\beta[q\psi_0(\mathbf{r})+\Omega r^2-\mu]\}}. \tag{3}$$

Here Ω and μ are constants to be determined by the conservation of total vorticity Q and angular momentum M,

$$Q=\alpha q=\int\omega_0d\mathbf{r},\quad M=\int r^2\omega_0d\mathbf{r}.$$

In the following sections we always scale parameters such that $q=1$ in our calculations.

III. SINGLE-VORTEX SOLUTIONS

Single-vortex solutions of the mean field equations in a disk include both symmetric vortices at the center and off-center vortices. Some properties of the symmetric solutions have been investigated in Ref. [7]. We will restate some of them here for completeness. For the calculation of symmetric solutions, the equations become

$$-\frac{1}{r}\frac{d}{dr}\left(r\frac{d\psi_0(r)}{dr}\right)=\omega_0(r)=\frac{q}{1+\exp\{\beta[q\psi_0(r)+\Omega r^2-\mu]\}}.$$

This equation can be numerically integrated with boundary conditions $d\psi_0/dr|_{r=0}=\psi_0(r=1)=0$. The values of μ, Ω, and β are determined from the required total vorticity, angular momentum, and energy by a standard root finding procedure.

For off-center vortices the partial differential equation, Eq. (3), must be solved. We use an iterative scheme to find the solutions. The space of the disk is discretized into a grid depending on whether a Fourier-finite difference or Fourier-Chebyshev expansion is used. The iteration starts with a estimated vorticity distribution $\omega_t(\mathbf{r})$. Naturally a circular vortex with a total vorticity approximately equal to the prescribed Q and a displacement from the disk center roughly consistent with the required M is used since we are interested in finding an off-center single-vortex solution. With this $\omega_t(\mathbf{r})$ we solve the Poisson equation $\nabla^2\psi_t=-\omega_t$. Next the ψ_t just calculated is substituted back into the right-hand side of Eq. (3) and we see that for each set of (μ,Ω,β) a new ω_t can be calculated. Again a root-seeking algorithm is used here to find the set of (μ,Ω,β) giving an ω_t with required Q, M, and E. Now the iteration can be repeated until a converged $\omega_t(\mathbf{r})$ is reached. We find that the method is robust and usually ω_t converges quickly to an off-center solution or to a symmetric one if the former does not exist. There are some variations of this method, e.g., β can be choosen initially and (μ,Ω) found for prescribed (Q,M), or S instead of E can be one of the fixed quantites.

Figure 1 shows the entropy as a function of energy for the symmetric and off-center vortices with $Q=0.2$ and $M=0.04$. Different values of Q and M yield similar results.

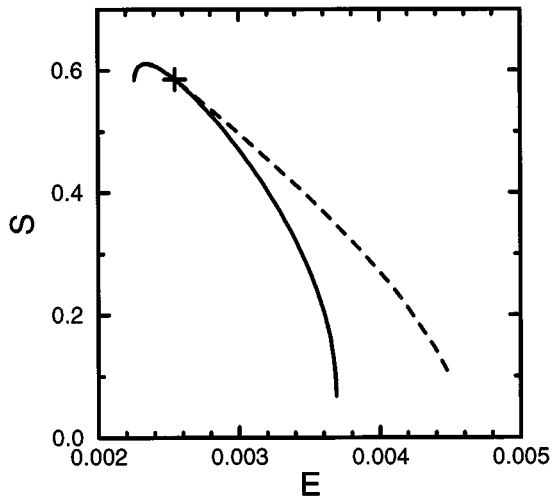

FIG. 1. Mean field solutions for $Q=0.2$ and $M=0.04$. Solid line: symmetric solutions; dashed line: off-center vortices; cross: bifurcation point.

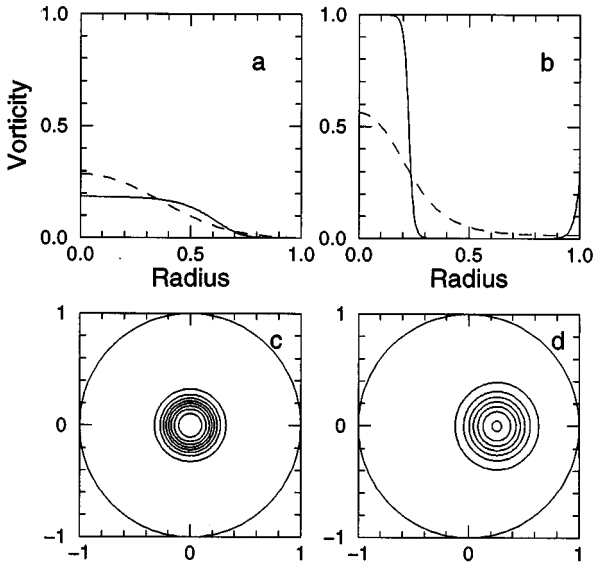

FIG. 2. Vorticity distributions for $Q=0.2$ and $M=0.04$ at various conditions. (a) Symmetric solutions at $\beta=1$ (dashed line) and $\beta=800$ (solid line). (b) Symmetric solutions at $\beta=-200$ (dashed line) and $\beta=-1000$ (solid line). (c) Vorticity contours for the symmetric solution at $E=0.003$. The contour levels start from 0.1 and increase by an interval of 0.1 toward the center. (d) Vorticity contours for the off-center vortex also at $E=0.003$, with the same contour levels as (c).

The energy or temperature can be considered as an indicator of how closely the vorticity is packed. The symmetric solution has a minimum energy limit, corresponding to $\beta\rightarrow\infty$, with $\omega_0(r)$ a uniform vorticity circular patch, shown as the solid line in Fig. 2(a), with its size and vorticity level uniquely determined by Q and M. It is interesting to note that in this case the size and level are independent of the $g(\sigma)$ constraint, i.e., the value of q in the current two-level vorticity special case. As the energy increases (β decreases) the vorticity level at the center rises [see Figs. 2(a) and 2(b)]. The entropy also increases but decreases again after passing the point $\beta=dS/dE=0$ and reaches zero at the high energy limit when $\beta\rightarrow-\infty$. At this limit the vorticity distribution saturates at level q and forms a circular vortex at the center and a vortex ring at the disk boundary, shown as the solid line in Fig. 2(b). The amount of vorticity in each region is determined by the angular momentum M. In this limit we would expect a single off-center vortex to have a higher energy because then all vorticity can stay together by adjusting the displacement from the center to satisfy the angular momentum constraint, and this is indeed shown by the solutions.

The distribution of the off-center branch at the maximum energy limit is an elliptical-like vortex with uniform vorticity q at a certain displacement D from the center. As the energy decreases, the entropy increases, the distribution of vorticity broadens, and the vortex moves toward the disk center. At a critical energy E_c, D becomes zero and two branches of solutions join together at the bifurcation point. At a fixed energy $E>E_c$ the off-center vortex always has a larger entropy than the symmetrical one; i.e., it is a more probable state. Contour plots of symmetric and off-center vortices at the same energy are plotted in Figs. 2(c) and 2(d), showing the off-center vortex is more diffusive than the symmetric one, yielding a higher entropy.

It is well known that a pure electron column in a high magnetic field behaves to a good approximation like a 2D ideal fluid. In Ref. [9] electron densities, equivalent to the vorticity distributions for a 2D ideal fluid, are studied for equilibrium electron columns. The quadrupole moment q_2 and rotational frequency f are measured for different vortex sizes and distances to center. The parameter q_2 measures the distortion of a vortex from a circular shape, and is defined as $(p_{xx}-p_{yy})/(p_{xx}+p_{yy})$, where $p_{xx}\equiv\int x^2\omega(\mathbf{r})d\mathbf{r}$ and similarly for p_{yy}, with (x,y) measured from the center of a vortex along the major and minor axes. We now compare our calculations with the experimental results. First we note that in the experiment the dependence of the behavior on the off-center displacement is studied for electron columns with similar size and internal distribution. To model this situation we observe that for the mean field solutions at fixed Q and β, different M values will give off-center solutions at different locations with very similar size and distribution. In this way we can have a good correspondence between the mean field solutions and experimental observed distributions.

For the three different values of the total vorticity used in the experiment, we plot q_2 versus D for β equal to -1000 (solid lines) and -200 (dashed lines) in Fig. 3. Calculations for an elliptical constant vorticity approximation [11] are also shown as the dotted lines. The vortices are very close to constant vorticity patches for the first β and have a smoother distribution for the second. First we see that for both β, the values of q_2 for a given total vorticity are close in all three cases. The likely physical reason is that the distortion comes mainly from the effect of the boundary (or in terms of the position of the image charge), and is mostly determined by the position of a vortex, not its detailed distribution. The measured q_2 from the experiment, shown as the symbols in Fig. 3, are consistent with our calculations. Although the electron columns have internal distributions closer to those of $\beta=-200$ than $\beta=-1000$, experimental errors make it

difficult to tell which line is closer to the experiment. This may also explain why the elliptical constant vorticity patch approximation shown as the dotted lines also gives consistent q_2 values. At small D the results are almost identical to the mean field solutions with the larger negative β but deviate from the experimental results when vortices come close to the boundary. On the other hand the mean field calculations describe correctly the trend of the experimental data at large D, with the solid lines seemingly better than the dashed lines.

IV. BIFURCATION ANALYSIS

The bifurcation from symmetric solutions to off-center vortices occurs at a critical energy and in principle we can understand the nature of the bifurcation and the behavior near it by computing all the solutions on the off-center branch. However, this is very time consuming [10] and there is always the uncertainty whether it is close enough to the bifurcation. Here we use a second-order perturbation analysis on symmetric solutions to investigate the bifurcation directly. Again, the mean field equation is

$$\omega(\mathbf{r}) = -\nabla^2\psi(\mathbf{r}) = \frac{q}{1+\exp[\beta(q\psi+\Omega r^2-\mu)]} \equiv h(\psi(\mathbf{r}),\beta,\Omega,\mu). \tag{4}$$

[Note that we drop the subscript 0 here for ψ and ω from Eq. (3).] We write a solution moving away from the symmetric branch at the bifurcation point onto the off-center branch as

$$\psi(\mathbf{r}) = \psi_0(r) + \delta\psi(\mathbf{r}) = \psi_0(r) + \epsilon\psi_1(r)\cos\theta + \epsilon^2[\psi_{2,0}(r) + \psi_{2,2}(r)\cos 2\theta] + O(\epsilon^3),$$

$$\omega(\mathbf{r}) = \omega_0(r) + \delta\omega(\mathbf{r}) = \omega_0(r) + \epsilon\omega_1(r)\cos\theta + \epsilon^2[\omega_{2,0}(r) + \omega_{2,2}(r)\cos 2\theta] + O(\epsilon^3),$$

$$\beta = \beta_0 + \delta\beta = \beta_0 + \epsilon\beta_1 + \epsilon^2\beta_2 + O(\epsilon^3),$$

$$\Omega = \Omega_0 + \delta\Omega = \Omega_0 + \epsilon\Omega_1 + \epsilon^2\Omega_2 + O(\epsilon^3),$$

$$\mu = \mu_0 + \delta\mu = \mu_0 + \epsilon\mu_1 + \epsilon^2\mu_2 + O(\epsilon^3).$$

Here we use subsrcipt 0 to indicate the symmetric state and ϵ is a small parameter. The $\sin\theta$ term at order ϵ is not included because it is degenerate with the $\cos\theta$ term due to the rotational symmetry. Substituting these expressions into Eq. (4) we get

$$\delta\omega = -\nabla^2\delta\psi = \sum_\alpha \left.\frac{\delta h}{\delta A_\alpha}\right|_0 \delta A_\alpha + \frac{1}{2}\sum_{\alpha\gamma}\left.\frac{\delta^2 h}{\delta A_\alpha \delta A_\gamma}\right|_0 \delta A_\alpha \delta A_\gamma + O(\delta A_\alpha^3).$$

Here A_α runs through ψ, β, Ω, and μ. Now we collect terms with the same power of ϵ and angular mode, and set them equal to zero separately. It also becomes apparent here that only $\psi_{2,0}$ and $\psi_{2,2}$ (and not $\psi_{2,1}$) are needed for the ϵ^2 term.

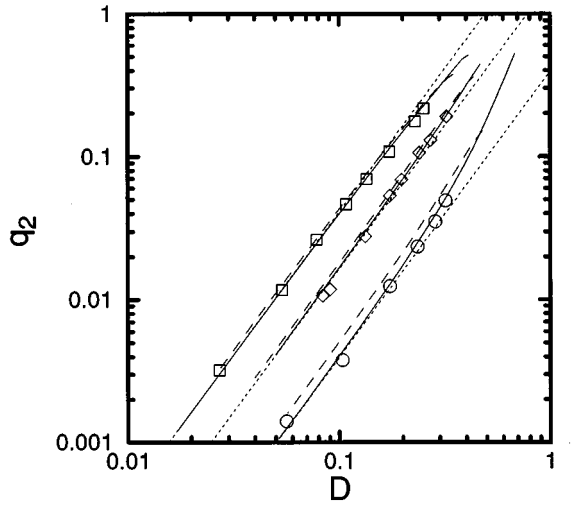

FIG. 3. q_2 as a function of D. The three groups of lines correspond, from top to bottom, to $Q=1.5837$, 1.0936, and 0.45365. Solid lines are the mean field solutions with $\beta=-1000$; dashed lines, $\beta=-200$. The dotted lines are the constant vorticity elliptical approximation. Symbols are the experimental results.

$$\epsilon: B_0\beta_1 + \beta_0 r^2\Omega_1 - \beta_0\mu_1 = 0,$$

$$\epsilon\cos\theta: (\nabla_1^2 - \beta_0 D_1)\psi_1(r) = 0, \tag{5}$$

$$\epsilon^2\cos 2\theta: (\nabla_2^2 - \beta_0 D_1)\psi_{2,2}(r) = -\tfrac{1}{4}\beta_0^2 D_2\psi_1^2, \tag{6}$$

$$\epsilon^2: (\nabla_0^2 - \beta_0 D_1)\psi_{2,0}(r) = -\tfrac{1}{4}\beta_0^2 D_2\psi_1^2 + D_1(B_0\beta_2 + \beta_0 r^2\Omega_2 - \beta_0\mu_2)/q, \tag{7}$$

$$\epsilon^3\cos\theta: (\nabla_1^2 - \beta_0 D_1)\psi_{3,1}(r) = G(r;\beta_2,\Omega_2,\mu_2). \tag{8}$$

Here,

$$\nabla_m^2 \equiv \frac{1}{r}\frac{d}{dr}\left(r\frac{d}{dr}\right) - \frac{m^2}{r^2},$$

$$B_0 \equiv q\psi_0 + \Omega_0 r^2 - \mu_0,$$

$$D_1 \equiv \omega_0(q-\omega_0),$$

$$D_2 \equiv \omega_0(q-\omega_0)(q-2\omega_0),$$

$$D_3 \equiv \omega_0(q-\omega_0)(q^2 - 6\omega_0 q + 6\omega_0^2),$$

$$G \equiv -\beta_0^2 D_2\psi_1(\psi_{2,0} + \tfrac{1}{2}\psi_{2,2}) + D_1\beta_2\psi_1 + \tfrac{1}{8}\beta_0^3 D_3\psi_1^3 - \beta_0 D_2\psi_1(B_0\beta_2 + \beta_0 r^2\Omega_2 - \beta_0\mu_2)/q.$$

The first equation just gives $\beta_1=\Omega_1=\mu_1=0$. The second one, Eq. (5), is an eigenvalue equation for $\psi_1(r)$. The solution will only exist for a particular value of β_0 and thus defines the bifurcation point of the symmetric state. After the bifurcation point β_0 and $\psi_1(r)$ are obtained, $\psi_{2,2}(r)$ can be calculated from Eq. (6). To solve for $\psi_{2,0}(r)$, we need three constraints to determine β_2, Ω_2, and μ_2 in Eq. (7). Two of them are given by requiring $\psi_{2,0}(r)$ to give no changes in the

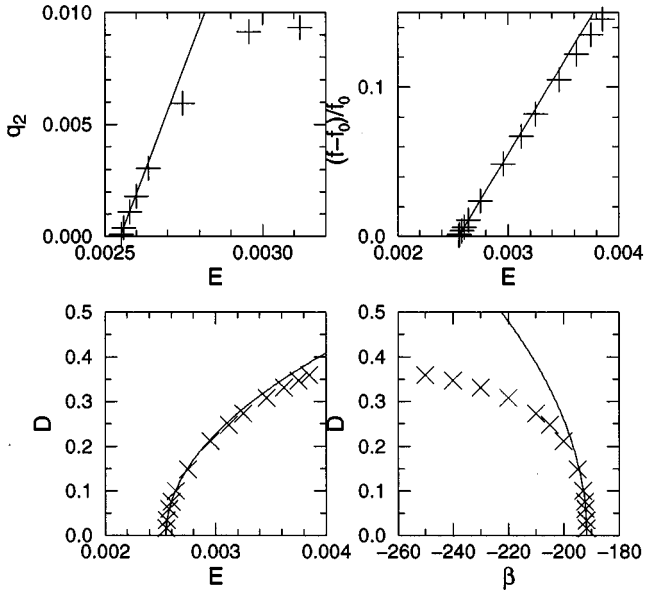

FIG. 4. Off-center vortex solutions for $Q=0.2$ and $M=0.04$. Solid lines: bifurcation analysis calculations; cross: off-center vortex solutions.

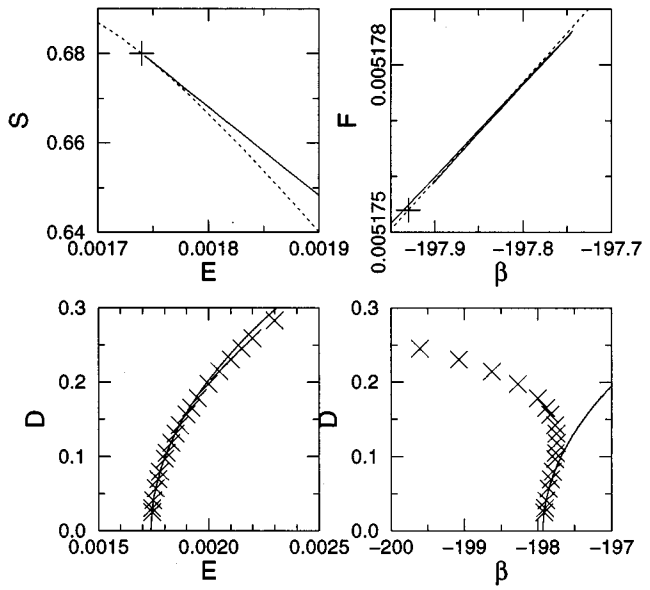

FIG. 5. Equilibrium states for $Q=0.2$ and $M=0.06$. In the upper two graphs, solid lines: off-center vortices; dotted lines: symmetric vortices; cross: bifurcation point. In the lower two graphs, solid lines: bifurcation analysis calculations; cross:off-center vortex solutions.

total vorticity and angular momentum. The third one comes from the solvability condition of the third-order equation, Eq. (8). Comparing Eq. (8) with (5), we see that

$$\int \psi_1(r)G(r;\beta_2,\Omega_2,\mu_2)rdr=0.$$

Combining these three constraints and Eq. (7) we can calculate $\psi_{2,0}(r)$, β_2, Ω_2, and μ_2. The properties of the off-center branch near the bifurcation can be easily computed from these solutions. For example,

$$D=\epsilon\pi\int \omega_1 r^2 dr \Big/ Q,$$

$$q_2=\left(\epsilon^2\pi\int \omega_{2,2} r^3 dr - QD^2\right) \Big/ (M-QD^2),$$

$$E-E_c=\epsilon^2 2\pi\int \psi_0\omega_{2,0}rdr+\epsilon^2\frac{\pi}{2}\int \psi_1\omega_1 rdr,$$

and rotational frequency shift $\Delta f\equiv(f-f_0)/f_0=\epsilon^2\Omega_2/\Omega_0$, with $f_0\equiv f(D\to 0)$.

The bifurcation point calculated from Eq. (5) is plotted as a cross in Fig. 1. We see that it agrees perfectly with the start of the off-center branch. In Fig. 4 we plot D, q_2, and Δf as functions of E or β for $Q=0.2$ and $M=0.04$. The solid lines are results from the bifurcation calculations and we find that the numerical solutions of off-center vortices, shown as crosses, agree well with the lines near the critical energy. If the displacement D is taken as the order parameter for an off-center state, its behavior clearly indicates a supercritical bifurcation. Thermodynamically we have a second-order (continuous) phase transition at E_c.

Interestingly for a larger value of M the situation changes. Bifurcation and off-center state calculation results are shown in Fig. 5 for $Q=0.2$ and $M=0.06$ (larger M yielding a larger vortex.) The D versus E curve is similar to the previous case, but now $\beta-\beta_c$ near the bifurcation [which is just $\epsilon^2\beta_2$ from Eq. (7)] is positive. Figure 5 indicates that we have a subcritical bifurcation when using the inverse temperature as the control parameter. Thermodynamically when the system is equilibrated at a fixed temperature, the transition to off-center vortices will be first order. The transition point β_f can be identified from the crossing of the solid and dashed lines in the free energy–inverse temperature plot. Although it may be difficult to see from the plot, in the small segment of the off-center branch near the bifurcation point (the portion with $dD/d\beta>0$), $d^2F/d\beta^2$ is negative. This leads to a negative specific heat and indicates the state is thermodynamically unstable at constant temperature.

The behavior becomes clearer when we plot the inverse temperature versus energy in Fig. 6. Considering the solid line in the inset, we see a typical equation of state for a first-order transition. The dashed line marks the temperature where the symmetric and asymmetric solutions have the same free energy: the transition will occur here as the temperature is varied. However, the usual interpretation of a system at the transition temperature as a mixture of two phases no longer applicable here due to the long range interaction between vortices. When a system at point A is fed energy by a heat bath at the same temperature, the system will not be in an equilibrium state until it gains enough energy to reach point B. If the contact with the heat bath is cut before reaching E_B, for example, at E_C, the system will relax to the equilibrium state C, which is stable in an isolated environment. Thus if the system energy is controlled continuously we have a continuous transition from symmetric to off-center states.

V. THERMODYNAMIC STABILITY

The mean field equations are obtained by requiring the vorticity distribution to be an entropy extremum. It remains

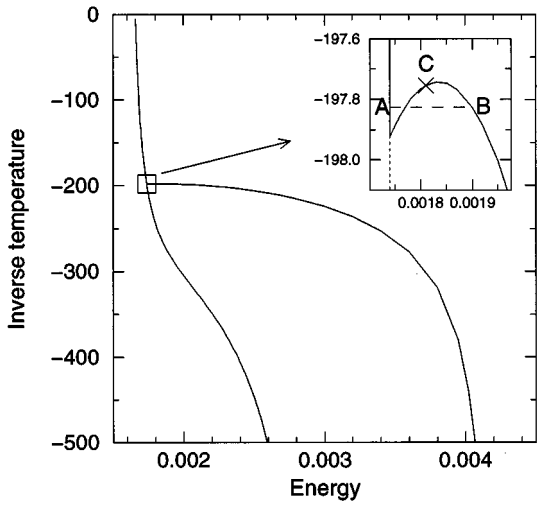

FIG. 6. β-E relation for the symmetric and off-center states with $Q=0.2$ and $M=0.06$. The line on the left is the symmetric solution; on the right the off-center vortex. In the inset the symmetric branch below the bifurcation point is drawn dotted and the horizontal dashed line marks the β where free energy of both branches cross in Fig. 5.

to be shown whether a particular solution is a maximum, minimum, or saddle point. From thermodynamics we know that the entropy must be a maximum for an equilibrium state to be stable. Consideration of the stability also helps us to understand the bifurcation. To determine the thermodynamic stability we add a small variation $\delta n(\mathbf{r},\sigma)$ to a solution $n_0(\mathbf{r},\sigma)$ and examine how the thermodynamic parameters change. This idea, with different implementation, has been used previously [6,8,12]. Here for a closed system with a fixed energy, we will examine the entropy change under the constraints of constant total vorticity, angular momentum, and energy. On the other hand for a system equilibrating with a heat bath at a constant temperature, the free energy will be studied with fixed Q, M, and β. Besides these thermodynamic contraints, all the infinite conservation laws of vorticity integrals should also be respected by δn. Since the state is already in equilibrium, the entropy or free energy will be evaluated up to second order in δn. In the current case of a two-level initial vorticity field, a small perturbation $\delta\omega(\mathbf{r})$ always satisfies the conservation of vorticity integrals. The changes in the total vorticity, angular momentum, and energy are

$$\delta Q=\int \delta\omega d\mathbf{r}, \quad \delta M=\int r^2\delta\omega d\mathbf{r},$$

$$\delta E=\int (\psi_0\delta\omega+\tfrac{1}{2}\delta\psi\delta\omega)d\mathbf{r}\equiv\delta E^{(1)}+\delta E^{(2)}.$$

The entropy change, up to the second order, is

$$\delta S=\beta\int \psi_0\delta\omega d\mathbf{r}-\int\frac{(\delta\omega)^2}{2\omega_0(q-\omega_0)}d\mathbf{r}\equiv\delta S^{(1)}+\delta S^{(2)},$$

and the free energy change is $\delta F=\delta S-\beta\delta E=\delta S^{(2)}-\beta\delta E^{(2)}$. For convenience our F differs from the usual free energy by a factor of $-\beta$. Note that in δF the linear terms from δS and δE cancel and we have a quadratic form left. For a closed system, because δE is required to be zero, we could use $\delta S-\beta\delta E$ instead of δS. Thus for both cases we will investigate $\delta S^{(2)}-\beta\delta E^{(2)}$ but the constraint $\delta E=0$ is required for a closed system as well as $\delta Q=\delta M=0$. In practice only $\delta E^{(1)}=0$ is needed because δS is only evaluated to second order.

To proceed we expand $\delta\omega(\mathbf{r})$ in a complete set of orthonormal functions $\phi_i(\mathbf{r})$: $\delta\omega(\mathbf{r})=\Sigma_i a_i\phi_i(\mathbf{r})$. Then δQ, δM, $\delta E^{(1)}$, and $\delta S^{(2)}-\beta\delta E^{(2)}$ can be expressed as

$$\delta Q=\sum_i Q_i a_i, \quad \delta M=\sum_i M_i a_i,$$

$$\delta E^{(1)}=\sum_i E_i a_i, \quad \delta S^{(2)}-\beta\delta E^{(2)}=\sum_{ij} S_{ij}a_i a_j.$$

Here Q_i, M_i, and E_i are vectors and S_{ij} is a matrix depending only on $\omega_0(\mathbf{r})$. Now we make an arbitrary linear transformation transforming a_i to b_i but requiring

$$b_1=\sum_i Q_i a_i, \quad b_2=\sum_i M_i a_i,$$

$$b_3=\sum_i E_i a_i \quad \text{(in the case of a closed system.)}$$

The constraints can now be satisfied with $b_1=b_2=0$ (or $b_1=b_2=b_3=0$ for a closed system.) In this new coordinate, S_{ij} changes to another matrix T_{ij} and $\delta S^{(2)}-\beta\delta E^{(2)}$ becomes $\Sigma_{ij>2(\text{or}3)}T_{ij}b_i b_j$. By removing the first two (or three) rows and columns from T_{ij}, we can perform the analysis without worrying about the constraints. If all eigenvalues of the new T_{ij} are negative, the state (ω_0,ψ_0) will be a free energy (or entropy) maximum. When the largest eigenvalue reaches zero as system parameters change, the state becomes a saddle point.

In the unit disk we expand $\delta\omega(\mathbf{r})$ in Fourier modes in the azimuthal direction and in Chebyshev polynomials in the radial direction:

$$\delta\omega(\mathbf{r})=\sum_{m=-\infty}^{\infty}\sum_{\substack{n=0\\ m+n=\text{even}}}^{\infty} a_{mn}T_n(r)e^{im\theta}.$$

Here $m+n$ even is required to give the correct parity for each m mode. When the calculation is applied to a symmetric distribution, the component a_{mn} separates for different m and every eigenvector has a definite value of m. The calculation is also faster because each m can be done separately. This is no longer true for an off-center vortex where all m modes are coupled together.

The largest eigenvalues of $m\leqslant 3$ for the symmetric solutions are shown in Fig. 7 for a closed system with $Q=0.2$ and $M=0.04$. For a fixed temperature system the $m=0$ eigenvalues will be different but the conclusions are similar. All eigenvalues are negative except for $m=1$ when the energy is larger than the critical energy obtained from the bi-

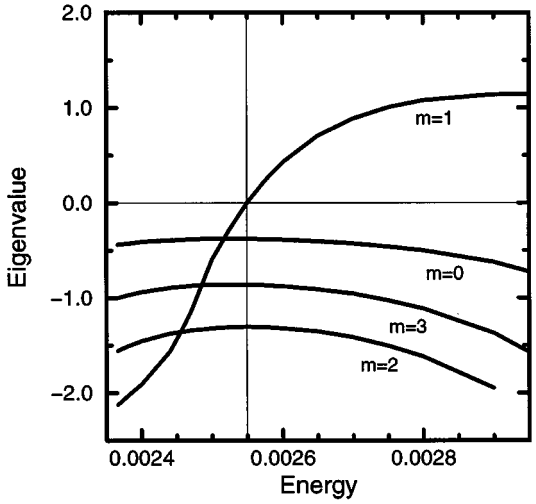

FIG. 7. Largest eigenvalues for symmetic solutions with $Q=0.2$ and $M=0.04$. The vertical line indicates the bifurcation energy.

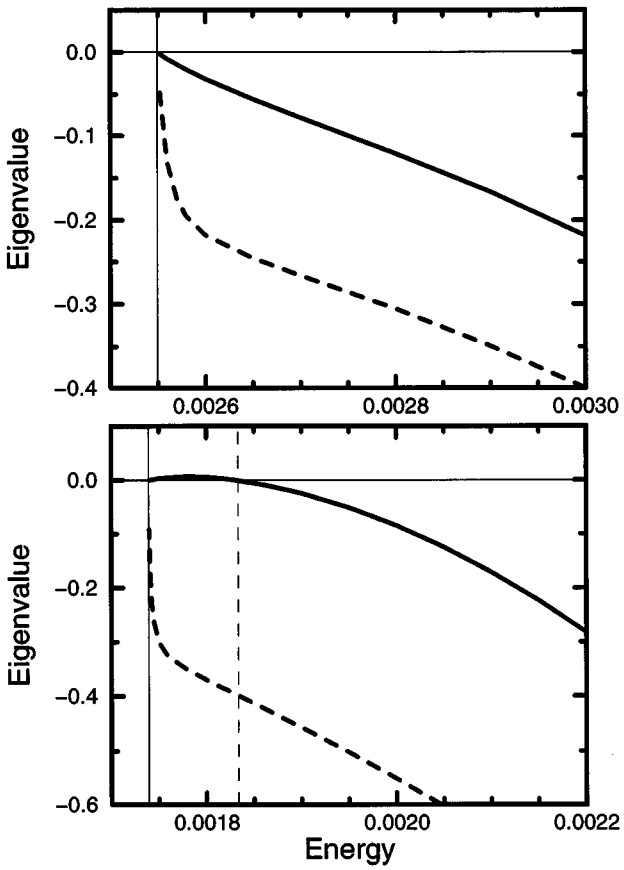

FIG. 8. Largest eigenvalues for off-center vortex solutions with $Q=0.2$. M equals 0.04 and 0.06 for the upper and lower graphs respectively. In both graphs, solid lines correspond to fixed β, dashed line to fixed E. The vertical solid lines indicate the bifurcation points; the vertical dashed line marks the beginning of the unstable segment calculated for the off-center solutions.

furcation analysis. This agrees with our calculations in previous sections in predicting that the symmetric states are stable below E_c. Above E_c the solution is no longer a local entropy maximum and the $m=1$ nature of the unstable eigenvector confirms that a bifurcation to an off-center vortex occurs.

Next we examine the stability of off-center vortices. For the case in Fig. 4 with a supercritical pitchfork bifurcation, it is natural to expect that these single vortices are stable. This is exactly the case as shown in the upper part of Fig. 8: all eigenvalues are negative and approach zero at E_c for both fixed energy and temperature cases. (There is actually a zero eigenvalue, not shown in the figure, because of the rotational degeneracy.) However, for $M=0.06$ at a fixed temperature, we have shown that the bifurcation is subcritical and we expect from the behavior of thermodynamic quantities that near the bifurcation the off-center branch is unstable. The solid line in the lower graph of Fig. 8 with a positive eigenvalue in this region explicitly shows that the states are not free energy maxima. On the other hand, when we consider a closed system we have all negative eigenvalues and this again agrees with the bifurcation analysis.

VI. CONCLUSIONS

In this paper the properties of the symmetric and off-center single vortices in a disk are calculated using the mean field theory of the Euler equations respecting the infinite number of conserved quantities. The comparison of the entropy of these solutions shows that the off-center vortices are thermodynamically more probable states than the symmetric vortices. The relation between the quadrupole moment specifying the degree of distortion from a circular shape and the vortex distance to the disk center agrees well with the result from an electron plasma experiment. The bifurcation from symmetric to off-center vortices is also investigated by a second-order perturbation analysis, which indicates the bifurcation is a supercritical (forward) pitchfork bifurcation when the system energy is used as the control parameter. On the other hand if temperature is controlled, a subcritical (backward) pitchfork bifurcation, and hence a first-order transition, will occur for some parameters. Our calculations of the thermodynamic stability of these solutions confirm these results.

The analysis we have presented is a local analysis around the stationary points of the mean field solution. However, since the stationary points that are stable are the asymptotic long time solutions from *any* initial condition with the prescribed values of the conserved quantities (at least ones leading to well mixed dynamics), the predictions have a global significance. The nature of the predictions is also quite different from given by a local stability analysis of the dynamical equations.

ACKNOWLEDGMENTS

We would like to thank Dr. K. S. Fine for providing us with their experimental data. This work is supported by the National Science Foundation under Grant No. DMR 9311444.

[1] J.C. McWilliams, J. Fluid Mech. **146**, 21 (1984), **219**, 361 (1990); W.H. Matthaeus, M.E. Brachet, M. Meneguzzi, H. Politano, and P.L. Sulem, *ibid.* **194**, 333 (1988); W.T. Stribling, D. Martinez, S. Oughton, and D. Montgomery, Physica D **51**, 531 (1991).

[2] K.S. Fine, A.C. Cass, W.G. Flynn, and C.F. Driscoll, Phys. Rev. Lett. **75**, 3277 (1995).

[3] P. Tabeling, S. Burkhart, O. Cardoso, and H. Willaime, Phys. Rev. Lett. **67**, 3772 (1991); O. Cardoso, D. Marteau, and P. Tabeling, Phys. Rev. E **49**, 454 (1994); D. Marteau, O. Cardoso, and P. Tabeling, *ibid.* **51**, 5124 (1995).

[4] See, e.g., L.J. Campbell and K. O'Neil, J. Stat. Phys. **65**, 495 (1991), and references cited therein.

[5] J. Miller, Phys. Rev. Lett. **65**, 2137 (1990); J. Miller, P.B. Weichman, and M.C. Cross, Phys. Rev. A **45**, 2328 (1992); R. Robert and J. Sommeria, J. Fluid Mech. **229**, 291 (1991).

[6] J. Sommeria, C. Staquet, and R. Robert, J. Fluid Mech. **233**, 661 (1991).

[7] P. Chen and M.C. Cross, Phys. Rev. E **50**, 2022 (1994).

[8] R.A. Smith and T.M. O'Neil, Phys. Fluids B **2**, 2961 (1990); T.M. O'Neil and R.A. Smith, *ibid.* **4**, 2720 (1992).

[9] K.S. Fine, C.F. Driscoll, and J.H. Malmberg, Phys. Rev. Lett. **63**, 2232 (1989).

[10] The convergence rate of the iteration becomes slower and slower as the solution gets closer to the bifurcation point.

[11] K.S. Fine, Phys. Fluids B **4**, 3981 (1992).

[12] P. Chen and M.C. Cross, Phys. Rev. E **53**, R3032 (1996).